Did Antarctic sea-ice expansion cause glacial CO_2 decline?

M. A. Morales Maqueda and S. Rahmstorf
Potsdam Institute for Climate Impact Research, Germany

Received 28 March 2001; revised 23 August 2001; accepted 5 September 2001; published XX January 2002.

[1] Recently, *Stephens and Keeling* [2000] have put forward an appealing theory for explaining the decrease in glacial atmospheric CO_2. They argue that a compact sea-ice cover extending southward of ~55° S trapped large amounts of CO_2 beneath the sea surface, thus accounting for the lower atmospheric concentrations. An atmosphere-ocean box model in which sea-ice area is prescribed allows them to simulate ~80% of the CO_2 drawdown. However, glacial CO_2 levels can be attained in their model only when the fraction of ice-covered area southward of the Antarctic Polar Front rises to 99–100%. We present simulations with a coupled sea ice-upper ocean model indicating that ice-area fractions so large might have not prevailed even under rather extreme glacial conditions. The combination of our glacial ice-coverage estimates with the ice area-CO_2 relation derived by Stephens and Keeling suggests that CO_2 sequestration under sea ice could account for at most 15–50% of the total glacial CO_2 decline. *INDEX TERMS:* 4267 Oceanography: General: Paleonography, 3344 Meteorology and Atmospheric Dynamics: Paleoclimatology, 4207 Oceanography: General: Arctic and Antarctic oceanography, 4255 Oceanography: General: Numerical modeling

1. Introduction

[2] Elucidating the causes of the glacial/interglacial atmospheric CO_2 cycles and their correlation with ice-volume and temperature changes [*Petit et al.*, 1999] is proving a most elusive problem. Depletion of surface nutrients at high latitudes is a favoured mechanism, but it is unclear to what degree such depletion occurred, and how much drawdown resulted from it [*Archer et al.*, 2000; *Sigman and Boyle*, 2000]. This has prompted some investigators to turn their attention toward physical processes that might exert a firmer control on atmospheric CO_2. It has recently been suggested that a drastic reduction in CO_2 outgassing over the Southern Ocean attending on a glacial expansion of the sea-ice cover could account for a substantial part of the 80–100 ppm decrease in CO_2 during the Last Glacial Maximum (LGM) [*Stephens and Keeling*, 2000] (hereafter SK).

[3] The theory of SK hinges upon the hypotheses that the bulk of the global deep water upwelling takes place southward of the Antartic Polar Front (APF), and that sea ice covered most of the upwelling region during the LGM. An atmosphere-ocean box model incorporating these two premises allowed them to reproduce a 65-ppm reduction in CO_2. However, their simulations reveal that sea ice-driven regulation of CO_2 outgassing is effective only if the wintertime sea-ice area fraction southward of the APF (hereafter A) is large: CO_2 drawdowns above 40 ppm necessitate values of $A \geq$ 95%, and their LGM case stipulates $A = 99.5\%$. The reason why sea ice is an inefficient barrier for air-ocean CO_2 exchanges lies in the following compensating mechanism. A positive ice-area anomaly causes both a decrease in atmospheric CO_2 and an increase in oceanic CO_2, leading to higher surface partial pressure differences, and hence to more vigorous CO_2 fluxes over the remaining open water area, thereby partly offsetting the effects of the initial perturbation. Because of this negative feedback, only a virtually locked, Arctic-like ice cover is able to reduce CO_2 concentrations down to glacial levels.

[4] Arguments have been put forward that vertical mixing increased during the LGM as a result of stronger surface cooling, ensuing sea-ice formation/salt rejection, and higher wind speeds [*Moore et al.*, 2000]. This would further weaken the sea ice-CO_2 link. Vertical mixing is a key factor in controlling CO_2 outgassing, since appreciable CO_2 release can occur only after the 50–300-m-deep surface layer has been brought into contact with the CO_2-rich underlaying waters. Upper ocean destratification during the LGM would have enhanced CO_2 exchanges over the more constricted open water areas.

[5] At present, strong circumpolar winds pull the ice apart, and intense oceanic heat fluxes hinder ice growth, to the point that sea ice covers no more than 80–90% of the total winter ice-pack area [*Gloersen et al.*, 1992]. The question naturally arises whether the harsher conditions that reigned during the LGM, notably lower air temperatures and faster winds, could have led to a nearly full sea-ice cover underneath which most of the Southern Ocean CO_2 would have been entrapped.

[6] Here, we examine simulations of a number of conceivable LGM scenarios carried out with a coupled sea ice-upper ocean model which suggest that the question above might need to be answered in the negative.

2. Model, Forcing, and Experiments

[7] The coupled sea ice-upper ocean model is that of [*Fichefet and Morales Maqueda*, 1997] (hereafter FMM). The ice model is a thermodynamic-dynamic one, and takes into account the heat capacity of snow and ice, the thermodynamic effects of the sub-grid-scale snow and ice thickness distributions, the storage of latent heat in brine pockets, and the formation of snow ice. It also allows for the dynamic creation and maintenance of leads within the ice cover (leads over a freezing ocean owe their existence exclusively to the motion of sea ice). The ice-dynamics formulation includes ice-ice plastic interactions. The upper ocean model consists of unconnected, 300-m-deep water columns incorporating parameterisations of the mixed layer and the diffusive pycnocline. The coupled model has a horizontal resolution of ~2.8° × 2.8°, and the ocean vertical levels vary in depth from 5 m at the surface to 50 m at the bottom.

[8] The following changes have been made from the initial FMM model. In FMM, an ad hoc redistribution of the heat flux through open water was applied to ensure that thermodynamic closure of leads did not occur. This artefact has been removed. The model uses now a physically-based formulation of the opening of leads by shearing deformation, a mechanism to be reckoned with for concentrations above 85–90% [*Stern et al.*, 1995]. In addition, we diagnose the collection thickness of new ice in leads as $d_l = d_0 + (2\, g\, \alpha\, (1 - \rho_i/\rho_w))^{-1}\, |\mathbf{u}_i - \mathbf{u}_f|^2$, where $d_0 = 0.1$ m is the thickness of frazil ice arriving at the edge of a lead, $g = 9.8$ m s^{-2}, $\alpha = 0.3$ is the volumetric fraction of frazil ice in water, $\rho_i = 950$ kg m^{-3} is ice density, $\rho_w = 1024$ kg m^{-3} is seawater density, $\mathbf{u}_i$ is the con-

0094-8276/02/2001GL013240$09.00

Table 1. Simulated wintertime mixed layer and sea-ice cover characteristics

Exp.	ΔT_a (°C)	Δv_g (%)	H_m (m)	A[a] (%)	$Å_d$[b] (%/month)	$Å_t$] (%/month)	D_l (m)	B_l (W/m^2)	D_{APF} (m)	V_{nAPF} (m/s)
PD	0	0	107	46.8 (282)	−1.5 − 0.1 = −1.6	2.6	0.7	−50	0	0
T05W00	−5	0	83	77.1 (270)	−2.6 − 0.6 = −3.2	3.5	0.7	−62	0.3	−0.001
T10W00	−10	0	117	93.7 (243)	−3.0 − 3.0 = −6.0	6.3	0.7	−130	1.9	0.017
T15W00	−15	0	145	95.4 (238)	−2.9 − 5.6 = −8.5	8.4	0.8	−211	3.3	0.029
T20W00	−20	0	154	96.6 (233)	−3.0 − 6.4 = −9.4	9.5	0.8	−302	4.4	0.032
T05W50	−5	+50	148	75.9 (271)	−3.6 − 1.0 = −4.6	4.9	1.0	−98	0.5	0.002
T10W50	−10	+50	174	92.3 (247)	−3.8 − 5.3 = −9.1	9.3	1.1	−218	3.0	0.029
T15W50	−15	+50	176	94.3 (242)	−4.1 − 6.7 = −10.8	10.6	1.1	−333	3.7	0.035
T20W50	−20	+50	180	95.6 (238)	−4.2 − 7.7 = −11.9	11.9	1.0	−461	4.5	0.039
T05W75	−5	+75	175	75.6 (271)	−4.0 − 1.4 = −5.4	5.6	1.2	−116	0.7	0.004
T10W75	−10	+75	192	91.0 (250)	−4.3 − 5.8 = −10.1	10.2	1.3	−255	3.3	0.033
T15W75	−15	+75	192	93.5 (244)	−4.6 − 7.1 = −11.7	11.5	1.2	−387	4.0	0.037
T20W75	−20	+75	195	94.9 (240)	−4.8 − 8.0 = −12.8	12.8	1.2	−531	4.6	0.041

[a] The figure in brackets is the atmospheric CO_2 concentration (in ppm) according to [*Stephens and Keeling*, 2000].
[b] The first (second) term on the left-hand side is the contribution to $Å_d$ from shearing deformation (ice divergence).

solidated ice velocity, and $\mathbf{u}_f = 0.06\ \mathbf{v}_g$ is the frazil ice velocity, with $\mathbf{v}_g$ the surface geostrophic wind [*Biggs et al.*, 2000]. This parameterisation returns values of d_l between ∼0.25 and ∼2 m.

[9] The model was integrated with boundary conditions representative of today's and LGM's climates. For the present-day climate simulation (PD), the seasonal cycles of surface heat fluxes, precipitation/evaporation rates, and wind stresses over sea ice and ocean are determined from monthly climatologies of atmospheric state variables, as in FMM. Ocean advection and horizontal diffusion of heat and salt are accounted for via restoring of the water column to annual mean data [*Levitus*, 1982]. At the base of the oceanic domain, heat and salt fluxes are set to zero, as their effects are implicitly included in the restoring.

[10] Available paleodata provide poor constrains on LGM boundary conditions. Of these, the most certain is insolation, which was lower than today by ∼14 W m^{-2} in late spring. However, imposing a seasonal cycle of LGM shortwave radiation anomalies on our model leads to virtually no alteration in winter ice-cover characteristics. Regarding deep ocean fluxes, a hypothetical cessation of the flow of North Atlantic Deep Water into the circumpolar region during the LGM would have removed ∼5–10 W m^{-2} from the oceanic sensible heat entering the mixed layer [*Crowley and Parkinson*, 1988]. For comparison, the heat-restoring flux in our model amounts to an annual input of ∼5 W m^{-2} into the oceanic area southward of the APF. With negative heat-flux anomalies of this magnitude, the simulated A experiences an increase of less than 10%, in agreement with the results of [*Crowley and Parkinson*, 1988]. Given the modest response of the ice cover to LGM shortwave and deep ocean-flux anomalies, we have formulated our glacial scenarios in terms solely of the LGM-minus-present differences in surface air temperatures and winds. We have performed 12 experiments, in each of which an annual mean air-temperature perturbation $\Delta T_a = -5, -10, -15$, or −20 °C, and a geostrophic wind-speed perturbation $\Delta v_g = 0$, 0.5, or $0.75 \times v_g$, are added to the present-day fields. These anomalies are within the range of current uncertainty [*Petit et al.*, 1999; *DeAngelis et al.*, 1987]. Oceanic advection and horizontal diffusion fluxes are prescribed from the restoring values determined in experiment PD. Model runs span 15 integration years.

3. Results

[11] The PD and LGM simulations are intercompared in terms of the following wintertime-mean quantities averaged over the area encircled by the APF: mixed layer depth (H_m), ice concentration (A), and rates of change of A as a result of ice-dynamics and lead-thermodynamics processes ($Å_d$ and $Å_t$, respectively). To support our analysis, we additionally consider the wintertime means of the collection thickness of new ice in leads (D_l), and the energy budget of leads (B_l), both of them averaged over the pack-ice region southward of the APF, and the average ice thickness and outward component of ice velocity along the APF (D_{APF} and V_{nAPF}, respectively). Table 1 displays the values attained by these variables in each simulation. We define wintertime as the 5-month period with highest ice-area fractions, and assume the APF to be delineated by the 3 °C annual mean sea-surface isotherm of [*Levitus*, 1982], which encloses an oceanic area of ∼32×10^6 km^2.

[12] Experiment PD reproduces well the modern sea-ice cover. As shown in Figure 1, the location of the simulated ice front (15% ice concentration) is close to the satellite-derived one [*Gloersen et al.*, 1992]. However, ice concentrations are overestimated all around Antarctica, and the mean ice compactness within the winter ice pack exceeds the observed value by ∼6% (84% vs. 78%). This discrepancy arises from the absence in our model of short term variability in the ice dynamics, such as that caused by inertial and tidal motions, whose contribution to wintertime lead formation is significant [*Eisen and Kottmeier*, 2000]. The simulated mixed layer is on average only ∼7 m shallower than inferred from [*Levitus*, 1982] based on a $\Delta\sigma_t = 0.125$ kg m^{-3} criterion.

[13] The experiment labelled T10W50 is our best guess LGM scenario, as it is the one with surface-temperature and wind-speed perturbations closest to those derived from the paleorecords. Figure 1c shows that the simulated ice front extends amply past the APF, and indeed also beyond the location of the LGM ice front estimated by CLIMAP [*Moore et al.*, 2000], suggesting that a glacial anomaly of $\Delta T_a = -10$ °C might, in fact, be too large, at least for latitudes above ∼55° S. In spite of the vastness of this ice cover, the average ice concentration southward of the APF reaches only ∼92%, which in the model of SK corresponds to a lowering of CO_2 by just 35 ppm. We also note that, as evidenced by the deepening of the mixed layer, vertical mixing is now stronger than in the PD case. An analysis of the complete set of LGM experiments will help understanding these results.

[14] The model's response in the sequence of LGM simulations exhibits a tidy pattern. For a given wind-speed perturbation, both A and H_m increase nonlinearly with decreasing air temperatures. The two quantities experience relatively large changes when the atmosphere cools down from $\Delta T_a = -5$ °C to $\Delta T_a = -10$ °C. For further temperature drops, however, fairly smaller increases occur (for H_m, this is most apparent at high wind speeds, since mixing is then mainly controlled by mechanical stirring). This nonlinearity is due to the fact that, barring heat transport through ice, net oceanic cooling is proportional to the area of leads, which decreases with decreasing T_a. Thus, if the ice concentration is 90%, say, a doubling of the surface heat fluxes will cause a meagre ∼20% increase in ice formation, salt rejection, and vertical mixing per oceanic unit area. It is worthwhile noting that, while lead-closure rates southward of the APF ($Å_t$) dominate lead-opening ones ($Å_d$) in the PD simulation, they come very close to be in balance in the LGM experiments. Of

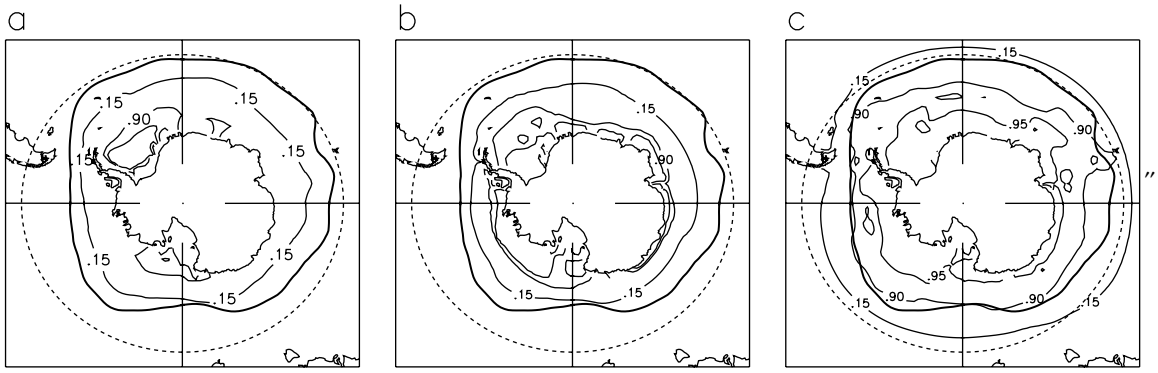

Figure 1. Wintertime sea-ice concentrations in the Southern Ocean from (a) SMMR observations, (b) the present day climate simulation, and (c) the LGM scenario where $\Delta T_a = -10$ and $\Delta v_g = 0.5 \times v_g$. Contour intervals are 0.15 (ice front), 0.90, and 0.95. The thick line delineates the mean path of the APF.

the two processes that add up to $\mathring{A}_d$, namely shearing deformation and ice divergence, changes in the latter are those that chiefly assist in establishing a closure/opening balance as air temperatures decrease. As is shown in Table 1, shearing deformation generates opening rates that, for a given wind speed, increase only weakly with ice concentration. In contrast, net ice-area divergence southward of the APF (i.e., total ice-area transport across the APF) rises significantly as air temperatures drop, thus neutralising the larger lead-closure rates. The increase in ice export across the APF results from the Coriolis intensification of the meridional component of the ice velocity as the ice, which by and large moves in free drift at those latitudes, grows thicker (cf. Table 1, last two columns).

[15] To ascertain the role of wind perturbations in controlling ice-area fractions, we first note that shearing deformation, ice divergence, and lead energy budget (column B_l in Table 1) are all three approximately proportional to wind speed. One would therefore expect changes in the wind to have only a lesser impact on A, were it not for the fact that the collection thickness of new ice tends to grow with v_g (roughly quadratically). As Table 1 reveals, the increase in ice collection thickness with enhanced winds creates a further mechanical hindrance to lead closure, which, for a given ΔT_a, results in a decrease in A as Δv_g augments. Note that lower winds during the LGM, as suggested by [*Sigman and Boyle*, 2000], would have led in contrast to an increase in fractional ice coverage.

4. Conclusions

[16] This investigation has been motivated by the conjecture of [*Stephens and Keeling*, 2000] that the glacial atmospheric CO_2 decay was caused by a reduction in outgassing rates over the Southern Ocean owing to a wintertime expansion and compaction (up to 99.5%) of the sea-ice cover. To assess whether the existence of such a compact ice cover is feasible in a LGM environment, we have carried out several integrations of the sea ice-upper ocean annual cycle in the Southern Hemisphere under boundary conditions representative of today's and LGM's climates. Despite the model's propensity to overestimating ice concentrations by several percents, the maximum value of the simulated ice-area fraction southward of the Antarctic Polar Front is ~95–97%, and our best guess LGM scenario yields a figure of ~92%. The persistence of relatively large amounts of open water within the ice pack stems from the alliance of three dynamical effects that tend to counter lead closure: shearing deformation and ice divergence, which promote lead opening, and wind-induced variations in the collection thickness of new ice, which decelerate lead closure. Our simulations show as well that the Southern Ocean mixed layer might have been up to ~90 m deeper during the LGM. Pressumably, the stronger oceanic vertical mixing would have supplied additional deep-ocean CO_2 to the surface, thus partly compensating for the increase in ice-area fractions. Inserting our simulated ice fractions into the ice area-versus-CO_2 concentration curve of [*Stephens and Keeling*, 2000], we estimate that entrapment of CO_2 by sea ice could account for not more than 15–50% of the glacial CO_2 decrease. Although it is implausible that Antarctic sea-ice expansion alone can fully explain the perplexing atmospheric CO_2 depletion during the LGM, our results do not discard sea ice as a potentially important control, one that might need to be considered, in conjuction with other mechanisms, by theories striving to solve the puzzle.

[17] **Acknowledgments.** The comments of E. Bauer, V. Brovkin, M. Hofmann, T. Kuhlbrodt, M. Montoya, and two anonymous reviewers are gratefully acknowledged. This work was supported by the German Ocean/CLIVAR Research Program.

References

Archer, D., A. Winguth, D. Lea, and N. Mahowald, What caused the glacial/interglacial atmospheric pCO_2 cycles?, *Rev. Geophys.*, *38*, 159–189, 2000.

Biggs, N. R. T., M. A. M. Maqueda, and A. J. Willmott, Polynya flux model solutions incorporating a parameterization for the collection thickness of consolidated new ice, *J. Fluid Mech.*, *408*, 179–204, 2000.

Crowley, T. J., and C. L. Parkinson, Late Pleistocene variations in Antarctic sea ice II: effect of interhemispheric deep-ocean heat exchange, *Clim. Dyn.*, *3*, 93–103, 1988.

DeAngelis, M., N. I. Barkov, and V. N. Petrov, Aerosol concentrations over the last climatic cycle (160 kyr) from an Antarctic ice core, *Nature*, *325*, 318–321, 1987.

Eisen, O., and C. Kottmeier, On the importance of leads in sea ice to energy balance and ice formation in the Weddell Sea, *J. Geophys. Res.*, *105*, 14,045–14,060, 2000.

Fichefet, T., and M. A. M. Maqueda, Sensitivity of a global sea ice model to the treatment of ice thermodynamics and dynamics, *J. Geophys. Res.*, *102*, 12,609–12,646, 1997.

Gloersen, P., et al., Arctic and Antarctic Sea Ice, 1978–1987: Satellite Passive Microwave Observations and Analysis, *SP-511*, 290 pp., NASA, Washington DC, 1992.

Levitus, S., Climatological Atlas of the World Ocean, *NOAA Prof. Pap. 13*, 173 pp., U. S. Gov. Print. Office, Washington DC, 1982.

Moore, J. K., M. R. Abbott, J. G. Richman, and D. M. Nelson, The Southern Ocean at the last glacial maximum: A strong sink for atmospheric carbon dioxide, *Global Biogeochem. Cycles*, *14*, 455–475, 2000.

Petit, J. R., et al., Climate and atmospheric history of the past 420,000 years from Vostok ice core, Antartica, *Nature*, *399*, 429–436, 1999.

Sigman, D. M., and E. A. Boyle, Glacial/interglacial variations in atmospheric carbon dioxide, *Nature*, *407*, 859–869, 2000.

Stephens, B. B., and R. F. Keeling, The influence of Antarctic sea ice on glacial-interglacial CO_2 variations, *Nature*, *404*, 171–174, 2000.

Stern, H. L., D. A. Rothrock, and R. Kwok, Open water production in Arctic sea ice: Satellite measurements and model parameterisations, *J. Geophys. Res.*, *100*, 20,601–20,612, 1995.

M. A. Morales Maqueda and S. Rahmstorf, Potsdam Institute for Climate Impact Research (PIK), PO Box 60 12 03, 14412 Potsdam, Germany. (maqueda@pik-potsdam.de)